

DESIGN FOR ADDITIVE MANUFACTURING: AN INVESTIGATION OF KEY MANUFACTURING CONSIDERATIONS IN MULTI-MATERIAL POLYJET 3D PRINTING

Nicholas A. Meisel and Christopher B. Williams
Design, Research, and Education for Additive Manufacturing Systems Laboratory,
Virginia Tech

REVIEWED

ABSTRACT

The PolyJet material jetting process is uniquely qualified to create complex, multi-material structures. However, there is currently a lack of understanding and characterization regarding important manufacturing considerations to guide designers in their use of the PolyJet process. This paper investigates key considerations necessary to ensure that proposed designs are manufacturable and that part properties are appropriate for the intended use. Considerations included in this paper include 1) minimum manufacturable feature size, 2) removal of support material from channels, 3) survivability of small features during water jet cleaning, and 4) the maximum self-supporting angle of printed parts in the absence of support material. The result of this work is an understanding of which geometric and process variables affect these manufacturing considerations. This understanding is crucial for the creation of a set of Design for Additive Manufacturing (DfAM) guidelines to help designers create ideal, manufacturable parts with less iteration and provide constraints for insertion into automated design processes such as topology optimization.

Keywords: Design for Additive Manufacturing (DfAM), PolyJet, 3D Printing, Multiple Materials, Material Jetting

1. DESIGN FOR ADDITIVE MANUFACTURING (DfAM)

Additive Manufacturing (AM) allows for the creation of parts of seemingly infinite complexity. While “complexity is free” for AM systems relative to traditional manufacturing technologies, there are still manufacturing constraints that must be considered when designing parts for AM. These manufacturing considerations vary between the different AM process types, with certain considerations playing a larger role in one process than in another. As an example, material extrusion processes must consider the significant material anisotropy that occurs in the layering direction, while direct metal processes must account for added support scaffolding and anchoring. As these constraints differ from traditional manufacturing processes, dedicated “Design for Additive Manufacturing” (DfAM) guidelines are needed to assist engineers in realizing products that make effective use of AM’s capabilities. A crucial component of these DfAM guidelines is identifying which geometric and process parameters will affect the manufacturing constraints (e.g., does layer thickness affect anisotropy in material extrusion parts?).

Modern automated design methods, such as topology optimization, can help engineers design parts that may have been almost unthinkable prior to the advent of AM. In fact, numerous researchers are investigating the use of topology optimization in the field of AM (see, for example [1–3]). An understanding of manufacturing considerations is necessary to ensure that these automated methods produce meaningful designs that can be accurately printed. At a basic level, this could be as simple as knowing the dimensions of the printer’s build volume to ensure that the algorithm cannot design a part that is larger than the machine can build. A more complex example is the incorporation of the anisotropic properties of printed materials in the analysis phase of topology optimization.

1.1. Establishment of a DfAM Framework

Several researchers are working to establish Design for Additive Manufacturing (DfAM) frameworks that will help designers to better account for the advantages and limitations of AM processes in their

designs. Rosen proposed a modified Process-Structure-Property-Behavior framework with a varying size scale [4]. The framework connects the behavior of parts back to key aspects of the manufacturing process. He utilized this framework to create a DfAM system for the creation of complex cellular structures. This framework is advantageous because the behavior, properties, and structure of a part can all be mapped back to the advantages and constraints of the manufacturing process used to produce it.

Hascoet and co-authors proposed what they termed a “global approach” to the incorporation of DfAM into printed parts [5,6]. Within this framework they suggest combining the functional requirements of the finished part with the manufacturing constraints of an AM process to develop a final geometry; this approach can be likened to the backward mapping that might occur from behavior to process in Rosen’s framework. The global approach is in contrast to the “partial approach” where a part’s geometry is designed beforehand and then adjusted to ensure manufacturability with AM. Hascoet cites work by Harzheim and Graf as a suitable example of this global approach. Harzheim and Graf combined the concept of topology optimization with the limitations of traditional metal casting (rather than AM) to create final parts directly from functional specifications and manufacturing constraints [7,8].

Maidin’s approach to DfAM relies more on detailed investigation of case studies than the more predictive analytic methods of Rosen and Hascoet. Maidin established a design feature database meant to spark inspiration in the designers hoping to use AM for creation of their products [9]. He looked to existing products from AM and attempted to distill their novel aspects into a taxonomy useable by those unfamiliar with AM (example features included “dual material products,” “internal structuring,” and “weight saving features”). Finally, Seepersad and coauthors used a similar experimental case study approach too establishing DfAM rules, but focused more on establishing clear quantitative inputs for DfAM. They performed a series of experiments to establish a designer’s guide for creation of holes, thin walls, text, and mating gears in the SLS process [10]. They created matrices to help provide guidelines for designers in common situations, e.g., a determination of how large embossed lettering should be in order to be legible when made via laser-sintering.

1.2. Context

An understanding of process constraints will be of benefit not only for assisting designers in preparing parts, but also in the creation of automated design tools that consistently provide manufacturable results. As already mentioned, topology optimization (TO) is one such tool. In essence, TO is an automated design methodology where a general design domain is defined (with associated forces, supports, and responses). Material is then systematically distributed in the space, according to a particular algorithm. The final result is a part that efficiently and effectively uses material to satisfy all constraints and maximize or minimize an objective function. More complex algorithms are able to incorporate various manufacturing considerations during the optimization process (see, for example, [11,12]). The goal of the research in this paper is to better understand the AM considerations that would need to be accounted for in such a manufacturing-oriented algorithm.

Due to its unique capability to produce multi-material parts and complex optimized structures through TO [13], the authors’ focus in this paper is in determining the process constraints of the PolyJet process. Specifically, the authors first identify four key PolyJet manufacturing constraints that could affect part design via TO (Section 2.3). The results of experimentation to identify the geometric and process variables that have a statistically significant effect on each of the manufacturing considerations is then presented. The four sources of process constraints are (i) support material removal (Section 3), (ii) minimum resolvable feature size (Section 4), (iii) feature survivability during cleaning (Section 5), and (iv) minimum self-supporting angle (Section 6). Motivation, experimental methods, results, and discussion are included for each of the four manufacturing considerations. Conclusions and recommendations for future work are offered in Section 7.

2. DFAM FOR POLYJET 3D PRINTING

2.1. PolyJet Overview

Of particular interest in this study is multi-material jetting (e.g., Stratasys' PolyJet technology), due to its ability to recreate fine geometric design features and its unique multi-material capabilities. Material jetting PolyJet printing is an AM material jetting process, wherein droplets of liquid photopolymer are deposited directly onto an elevator via a series of inkjet printheads [14]. As the material is deposited, two ultraviolet (UV) lamps cure the photopolymer in multiple passes. Each subsequent layer is jetted on top of the previous one. A representation of this process can be seen in Figure 1.

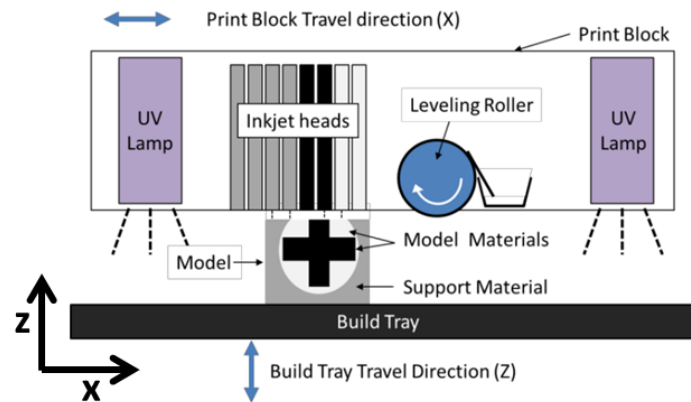


Figure 1. Representation of Direct 3D PolyJet Printing Process

The PolyJet process is able to create small features as it has a layer thickness of 16-32 microns and an in-plane resolution of 42 microns. In addition, the PolyJet process offers one significant, unique advantage among modern additive manufacturing process: the PolyJet process is capable of depositing two different materials on a pixel-by-pixel basis. This allows for creation of monolithic structures from multiple materials in a single build. One material combination of engineering relevance is VeroWhite+, a rigid, white plastic-like material, and TangoBlack+, an elastomeric, flexible black material. The two materials can be combined in various ratios to create nine gradient material blends with elastic modulus properties ranging along the continuum of the two extremes. The Polyjet process also uses a sacrificial, hydrophobic support material during part creation. After printing, this gel-like photopolymer must be manually removed using the recommended water jet cleaning station.

2.2. Prior Characterization of PolyJet

No researchers have yet created a detailed guide of DfAM considerations for the PolyJet process. Likewise, few have attempted to determine the effects that the PolyJet's various parameters (printhead resolution, support material usage, multi-material options, etc.) have on these considerations. A review of existing work shows that i) existing studies tend to focus on material characterization, ii) process/property relationships have not been fully explored, and iii) the key process constraints of PolyJet have yet to be identified.

Regarding material characterization, Moore and Williams investigated the fatigue life of the elastomeric TangoBlack+ material produced by the PolyJet process [15]. They were able to create an experimental curve relating the percent elongation of a TB+ specimen to the expected life of the specimen. They also derived several design rules from their study; one example is to avoid necks in a designed part, since necks were found to reduce the fatigue life of specimens. Pilipovic and co-authors measured the tensile and flexural properties of VeroBlack, VeroBlue, and Fullcure 720 materials; they found that the Fullcure 720 performed the best of the three, with a flexural strength slightly higher than the manufacturer's quoted value [16]. The Fullcure material was also found to have a tensile strength lower than the manufacturer's cited value. Vieira and co-authors found that the flexural modulus of Fullcure 720 can be further improved through UV or thermal post-processing, though this also has a

negative effect on fatigue life [17]. Finally, Gibson and coauthors investigated the elastomeric properties of Fullcure 720 in both compression as well as bending [18]. Their experimentation showed that, while the material can be used for the creation of “living hinge” designs, its elastomeric properties are not strong enough to withstand heavy use.

In addition to material characterization, there has also been some prior work into characterizing the PolyJet process and its effect on final parts. Udriou investigated the surface finish of parts made of Fullcure 720 and found that the machine’s glossy surface finish setting gave parts a much lower surface roughness than the matte setting [19,20]. He also performed a basic investigation into how build time and material consumption changes relative to part orientation. From this investigation, he was able to provide several guidelines for optimal part orientation (e.g., “the smallest dimension along z-axis” and “highest part to the left”). Singh likewise characterized the material consumption and build time of a nominal test part with the PolyJet process and confirmed Udriou’s claim that the largest part dimensions should be aligned in the X-axis [21,22]. In addition, he investigated the dimensional accuracy of the part when built in different orientations and found that the x-axis orientation also offered the best dimensional accuracy for parts.

Kim and Oh also offer an investigation of PolyJet material and system characterization. In their paper, they investigate numerous properties of manufactured PolyJet parts [23]. The authors discovered a 50% decrease in PolyJet tensile strength in the z-direction of parts compared to the x-direction. They also discovered that the tensile strength of PolyJet parts decreases steadily and significantly as temperature is increased. While Kim and Oh did investigate minimum feature size, one of the goals of the research proposed in this paper, they did so only with simple rib and rectangular/circular gap shapes in a glossy finish. These shapes are capable of providing a benchmark minimum feature size, but may not capture the variation in size that may come from alternate orientations, surface finishes, and feature shapes (for example, the droplet-based nature of the PolyJet may allow it to recreate positive circular features more effectively than rectangular ones).

Investigation of the properties at the interface of disparate printed materials is one of the potential key focuses of PolyJet research. In addition to their study of general PolyJet material fatigue life, Moore and Williams also investigated the effect that the presence of a sharp material interface would have on the fatigue failure location of a test specimen [15]. They found that having a sharp interface between TangoBlack+ and VeroWhite+ loaded in shear would almost always cause the specimen to fail at the interface (92% of their specimens failed at the shear interface while only 8% failed at the weaker TB+ material). However, despite being a central tenet behind the creation of PolyJet parts, the multi-material interface is still generally under-investigated in existing literature.

As this review demonstrates, PolyJet characterization research has included some investigation into manufacturing considerations such as material anisotropy and feature size. However, each of these studies tend to focus on one or two constraints and investigate the effects of only one variable on the constraints. A broader approach is needed to establish a larger field of PolyJet manufacturing constraints and to identify the essential process/geometry variables for each constraint. The experimental methods (Sections 3-6) of this work seek to fill this gap in understanding.

2.3. Identification of PolyJet Manufacturing Considerations

To illustrate the importance of manufacturing constraints when combined with topology optimization, consider the optimized compliant inverters from [13] (Figure 2). Both were designed using TO methods and subsequently printed via PolyJet AM.

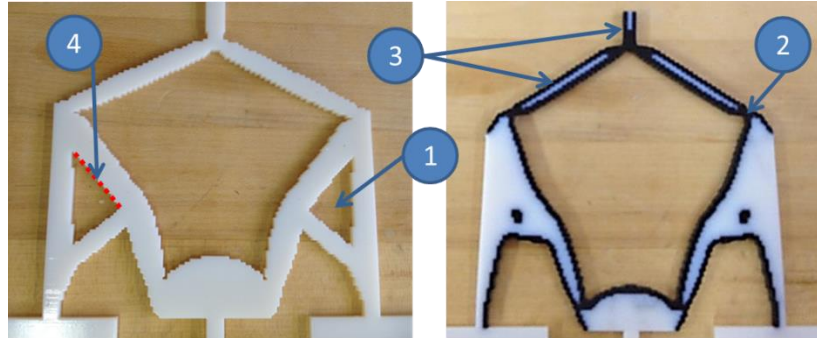


Figure 2. Optimized Compliant Inverters Manufactured via PolyJet AM [13]

While the geometry of these inverters is relatively simple, they nevertheless help to illustrate certain concerns and possibilities that may arise in the use of automated design tools in AM. These potential manufacturing constraints are identified as follows (note that the callouts in Figure 2 match the numbering below):

1. **Support Material Removal:** Depending on part orientation and surface finish, the triangular holes in the single-material specimen would be filled with the PolyJet process’s hydrophobic support material. It is necessary to ensure that these holes are large enough to allow for rapid, manual removal of the support material during cleaning.
2. **Minimum Feature Size:** In the case of the compliant inverter design domain, the TO algorithm tends to create narrow, hinge-like sections in the final design in order to increase deflection at the tip. Knowing the minimum manufacturable feature size in the PolyJet process, and incorporating that value into the TO formulation, will allow these joints to be as small as possible. This in turn will increase the maximum deflection of the inverter.
3. **Survivable Feature Size:** As mentioned, PolyJet support material must be removed manually with a high-pressure water jet. Experience shows that it is possible for smaller features (such as the long, thin arms and tip of the inverter) to break during the cleaning process. Because of this, it is crucial to determine the factors that drive part breakage and establish the minimum feature size that can survive the cleaning process.
4. **Self-Supporting Angle:** To remove any concerns about support cleaning or feature survivability, it is possible to completely eliminate support material use in the creation of PolyJet parts. By doing this, it becomes necessary to ensure that angled faces (such as the one highlighted with the dashed line) will not collapse without support material. This can be predicted by determining the self-supporting angle of angled faces.

The experimentation that follows in the remainder of this paper will focus on identifying the geometric and process variables that have a statistically significant effect on these four manufacturing constraints. Without first understanding which parameters have an effect on the constraints, it is difficult (if not impossible) to establish a robust set of quantitative DfAM relationships to incorporate into TO.

3. SUPPORT MATERIAL REMOVAL

3.1. Motivation

As mentioned in Section 2.1, the PolyJet process uses a hydrophobic, gel-like photopolymer as a secondary sacrificial support material. As in other AM processes, this support material is used to ensure overhanging and angled structures are built properly (as was mentioned in reference to the triangular gaps in Figure 2). As the support material also affects a part’s surface finish, the PolyJet process offers two surface finish options during pre-processing: selecting the “matte finish” provides a uniform surface finish to the part by coating every surface in support material (even top-facing surfaces); selecting the

“glossy finish” only provides support material to overhanging features (typically resulting in the top-facing surfaces having a more glossy finish than the remainder of the part). This support material is then removed manually with small tools or with a high-pressure water jet. The need to manually remove support material places significant limitations on the final geometry from an automated design process. Any fully enclosed cavities will be filled completely with support material that cannot be removed. In addition, certain long, narrow cavities may be difficult to clean.

The experiments described in this section are designed to answer the question, *What process parameters and geometric features affect the ability to successfully remove support material from printed parts?*

3.2. Experimental Methods

While no research has been done in support material removal specifically for the PolyJet, Vayre and coauthors began an experimental investigation into the cross-sectional size necessary to remove powder support material from channels in parts manufactured with electron beam melting [24,25]. They used compressed air to remove loose support powder from cylindrical channels of varying diameters and measured the depth of powder removed after a specified period of time. They found that as the cross-sectional area of a channel was increased, the depth of powder removed from it also increased. They also noticed a qualitative difference between the channel geometry and how much powder was removed (cylindrical tubes were more easily cleaned than square ones). Of note is that the authors mention the need to avoid fully enclosed internal cavities due to the presence of support material, which is a consideration that would be important to account for in automated design methods.

A similar experiment is performed here where the PolyJet support material is removed with a water-jet. The support-filled channel specimens for this experiment rely on variation of three independent variables: (i) channel geometry, (ii) channel cross-sectional area, and (iii) channel connectivity (open at both ends or closed at one end). These geometry and cross-sectional area variables are included since they were found to have importance by Vayre and coauthors, while connectivity is a new inclusion based on our existing knowledge of the PolyJet cleaning process. Each variable, its two states, and its associated hypothesis are presented in Table 1. For this experiment, the length of the channel is held constant (at an arbitrary length of 44.2 mm) as is the total cleaning time (set at 2 minutes). An example of the test specimens is shown in Figure 3. Two iterations of each chosen variable combination were tested.

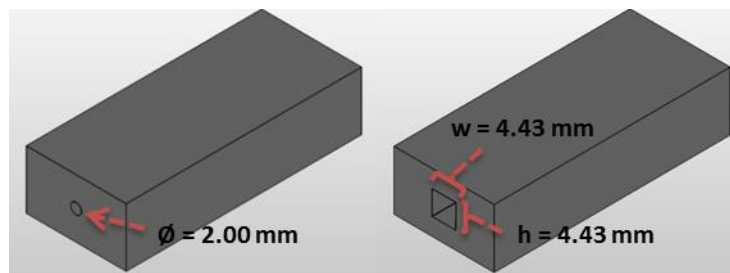


Figure 3. Example of Support Cleaning Test Specimens

Table 1. Experimental Variables in Support Material Removal

Independent Variables			
Variable Name	State 1	State 2	Rationale/Hypothesis
Cross-Sectional Geometry	Circle	Square	Support material may prove more difficult to remove from the sharp corners of a square cross-section.
Cross-Sectional Area	3.14 mm ²	19.64 mm ²	It may prove more difficult for the water stream to break away the support material in a smaller area.
Connectivity	Closed	Open	If the channel is closed at one end, support material may be removed more slowly since it will only have one exit point.
Dependent Variable			
Variable Name	Units		Rationale
Support Material Removed	% (by mass)		Measuring the percent mass of support material removed will help to determine the variables that slow the cleaning process (or impede it entirely).

To facilitate careful and consistent cleaning practice, a test rig was designed to maintain a constant distance and angle from the support-filled channels using a constant water pressure of 1750 psi (Figure 4). The specimens were each cleaned for two minutes using this rig; the amount of support material removed was then calculated.

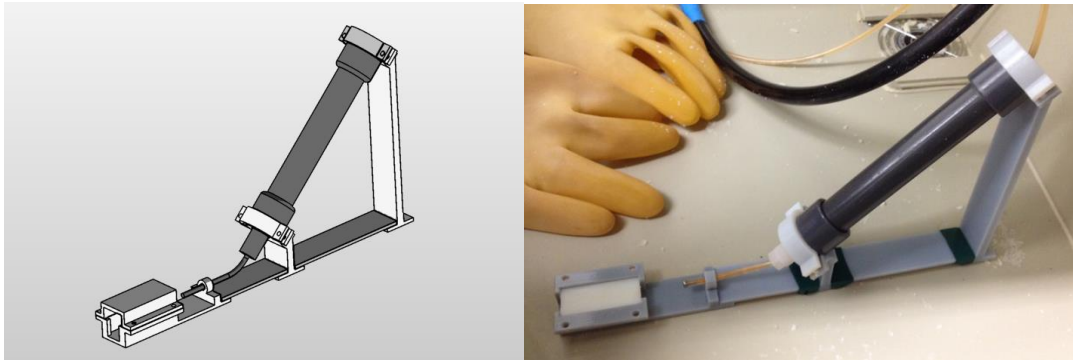


Figure 4. Cleaning Test Rig

To determine the amount of support material that is removed in each test specimen, an initial piece with known support volume, model volume, and model density is weighed to calculate the density of support material. The total percent of support material removed is determined by comparing the mass of the experimental specimens before and after cleaning. This metric is used to represent the ease of removal of support material for a given geometry; the higher the percentage of support material removed at the end of the two minutes, then the easier the geometry is to clean.

3.3. Results

ANOVA analysis was performed on an L8 Taguchi array with two iterations of specimen cleaning. The average amount of support material removed across all specimens was 25.4% (by mass, seen in Table 2). This value offers a general benchmark of how much support material is removed at this particular time/size scale, but does not offer much information regarding the roles of the independent variables. The results in Table 3 offer more detail about the role of each variable. The information in the table suggests that only the cross-sectional area of the cleaning specimens affects the amount of support material removed in a fixed amount of time; it is the only variable with a p-value < 0.05. Using the larger cross-sectional area results in a higher percentage of support material removal, as hypothesized, with an approximate increase of almost 12% over the smaller cross-section. However, it is worth noting the relatively low R² value when compared to the other experiments in this paper (0.742, from Table 1). Figure 5 shows the desirability predictions based on the ANOVA analysis; the square cross-section, larger cross-sectional area, and closed channel configuration is predicted to offer the highest percentage

of support material removed (though, again, only the cross-sectional area is deemed statistically significant).

Table 2. Summary of Fit – Support Cleaning

RSquare	0.742
Root Mean Square Error	5.301
Mean of Response	25.409
Observations (or Sum Wgts)	8

Table 3. Parameter Estimates – Support Cleaning

Term	Estimate	Std Error	t Ratio	Prob> t
Intercept	25.409	1.874	13.56	<.001*
Geometry[Circle]	-2.331	1.874	-1.24	0.282
Cross-Sectional Area[1]	-5.903	1.874	-3.15	0.035*
Connectivity[Closed]	0.233	1.874	0.12	0.907

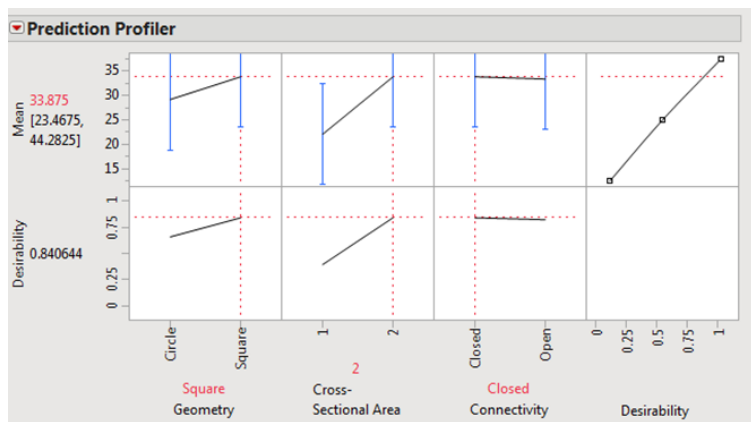


Figure 5. Desirability Prediction – Support Cleaning

3.4. Discussion

The result that suggests that increased cross-sectional area providing easier support material removal aligns with intuition, as well as the results found by Vayre and coauthors. However, it is surprising to see that connectivity may play no part in support material removal (according to the ANOVA analysis). It is possible that the connectivity would play a larger role if cleaning time was also accounted for as an independent variable; as more material is removed, the water stream will reach the other end of the channel, which may increase the observed effect of the connectivity.

4. MINIMUM RESOLVABLE FEATURE SIZE

4.1. Motivation

Every AM process has a limit on the smallest feature that it can create. This is most closely tied to the size of the deposition nozzle (or beam diameter, or particle size), the layer thickness, and the resolution of the x, y, and z direction motors in the printer frame. Stratasys specifies that the PolyJet process has a resolution of 42 micron in the x- and y-directions with a layer thickness between 16 and 32 microns. However, it is necessary to validate how these quoted resolution values influence the smallest feature size that can be printed (which in turn relates back to the thin hinge like sections in the inverters from Figure 2). While there has been some preliminary investigation into this with simple single-material rib shapes, as seen in [23], it is important to understand if the minimum manufacturable feature size differs between VeroWhite+ and TangoBlack+ material, surface finish types (denoted in the printer

as “matte” vs. “glossy”), part orientation, feature direction (embossed or debossed), and feature geometry.

The experiments described in this section are designed to answer the question, *What process parameters and geometric features affect the smallest part feature size that can be created by PolyJet?*

4.2. Experimental Methods

A standardized test specimen has been proposed by authors from NIST for use in characterizing the products of AM processes (Figure 6) [26]. Each feature of the specimen is meant to directly relate back to an aspect of the manufacturing process (e.g., resolution of the XY motors, layer thickness, etc.). This specimen includes both rectangular and circular features to quantify the minimum feature size of the AM machine. These minimum feature aspects will inform the design of our own minimum feature specimen, created solely to investigate the PolyJet process’s ability to create small embossed and debossed features.

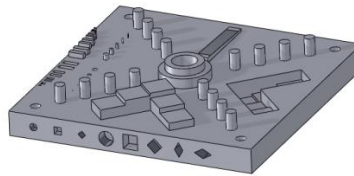


Figure 6. AM Feature Specimen Proposed by NIST [26]

As the high resolution of the PolyJet process is one of its primary advantages, there was concern over whether or not the NIST specimen would be small enough to identify the uniquely high resolution of the PolyJet AM process. As such, a specimen was designed which maintains the same geometry as the NIST specimen, but utilizes even smaller lower limits on the feature geometry being printed. In addition, it uses significantly less material than the NIST specimen, which facilitates efficient experimental repetition. The specimen design, seen in Figure 7, has been divided into quarters; one quadrant of the specimen is printed based on what type of feature is being tested.

The independent variables for this experiment include (i) material type, (ii) surface finish, (iii) orientation, (iv) feature direction, and (v) feature shape. These variables, their two states, and the hypothesis associated with each are shown in Table 4. The dependent variable is the minimum feature recreated by the PolyJet process. All specimens were cleaned using an Objet-recommended water-jet station with a pressure of 1750 psi. Two iterations of each tested variable combination were performed.

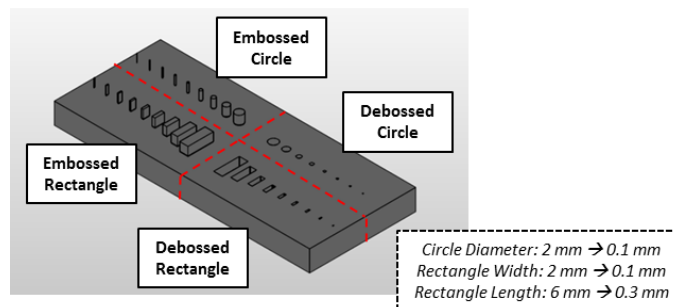


Figure 7. Minimum Feature Specimen

Table 4. Experimental Variables in Minimum Resolvable Feature Size

Independent Variables			
<i>Variable Name</i>	<i>State 1</i>	<i>State 2</i>	<i>Rationale/Hypothesis</i>
Material Type	TB+	VW+	The compressive force of the roller may deform small features in the flexible TB+ during printing, hampering creation of smaller features.
Surface Finish	Glossy	Matte	The extra support material required for the matte surface finish may better support smaller embossed features and maintain the geometry of smaller debossed features.
Orientation	XY	XZ	The PolyJet's Z-resolution of 32 microns is actually finer than the X-Y resolution of 42 microns, so smaller features may be possible in the XZ orientation.
Feature Direction	Debossed	Embossed	The compressive force of the roller may damage embossed features during printing (but cannot damage debossed features). Cleaning may also damage smaller embossed features.
Shape	Circle	Rectangle	The droplet-based deposition pattern of the PolyJet process may have difficulty recreating the sharp corners of rectangular cross-sections at small feature sizes.
Dependent Variable			
<i>Variable Name</i>	<i>Units</i>		<i>Rationale</i>
Minimum Feature Size	mm		Measuring the minimum feature size will determine the smallest feature allowed in an automated design algorithm.

4.3. Results

ANOVA analysis was used on a L12 Taguchi array to determine which of the independent variables has the greatest impact on the minimum resolvable feature size. A feature was considered resolvable if it maintained the true nature of the cross-sectional shape (e.g., rectangles had 4 distinct linear sides) and was of the same height as the other specimens (though this is difficult to validate with the debossed features, since measurement tools will not fit inside the extrusions). Because the minimum feature size was determined by human interpretation (with the assistance of a digital microscope), it is possible that the final statistical data might vary from observer to observer. Statistically significant values are denoted with an asterisk.

From this data, the mean resolvable feature size is approximately 0.73 mm (Table 5). As with the average value from the support removal experiments, this number simply offers an approximate benchmark accounting for changes to all independent variables. More importantly, the results of experimentation show two statistically significant factors that contribute to the minimum PolyJet feature size. Shown in Table 6, these are the print material (VW+ or TB+, with a p-value of 0.002) as well as the feature direction (embossed or debossed with a p-value of 0.003). Print material has the greatest effect on feature size (potentially causing a change of 0.330 mm from one material to the other) while the feature direction has the second greatest effect (with a magnitude of change of 0.288 mm between debossed and embossed features). Both of these values can be derived from the estimates in Table 6. The desirability predictions shown in Figure 8 predict that the smallest feature will be created with a combination of embossed VW+ material, a glossy surface finish, an XY orientation, and a rectangular shape.

Table 5. Summary of Fit – Minimum Feature

RSquare	0.904
Root Mean Square Error	0.106
Mean of Response	0.731
Observations (or Sum Wgts)	12

Table 6. Parameter Estimates – Minimum Feature

Term	Estimate	Std Error	t Ratio	Prob> t
Intercept	0.731	0.031	23.98	<.001*
Material[TB+]	0.165	0.031	5.40	0.002*
Surface Finish[Glossy]	-0.035	0.031	-1.16	0.290
Orientation[XY]	-0.035	0.031	-1.16	0.290
Extrusion Direction[Debossed]	0.144	0.031	4.71	0.003*
Shape[Circle]	0.048	0.031	1.57	0.167

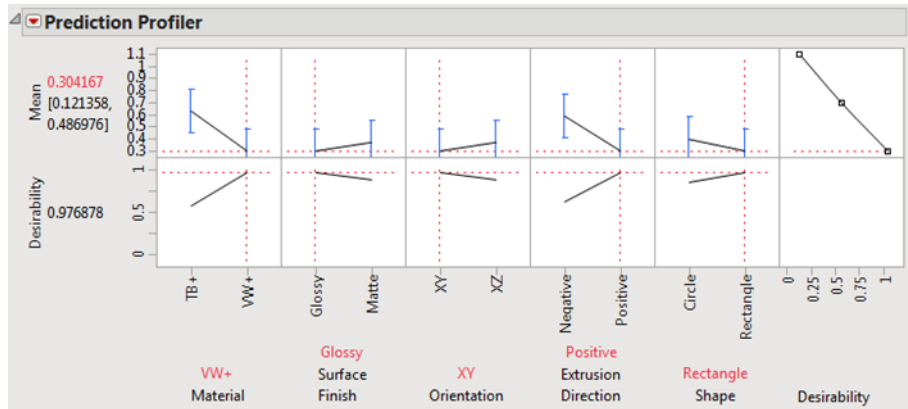


Figure 8. Desirability Prediction – Minimum Feature

4.4. Discussion

Much was learned from observing the printed minimum feature specimens underneath the digital microscope. VeroWhite+ material proves to be most beneficial because it creates much more clear and defined geometry in small features than TangoBlack+ (the spongy nature of TB+ has a tendency to blur the boundaries of small features). In addition, XZ-oriented specimens had features which appeared “squashed” when viewed under a microscope (e.g., circular cross-sections appeared as ovals). This is most likely an effect of the poorer XY resolution discussed earlier; the resolution causes the dimensions of the circular cross-section to be manufactured larger in the X-direction, giving the squashed appearance.

As discussed earlier in Section 1.2, the force of the waterjet cleaning tends to break smaller parts. Even though the embossed features still performed better than the debossed features, this type of breakage can be seen very clearly in these minimum feature size specimens. Specimens with matte, embossed features are especially susceptible to breakage, since there is more support material that needs to be removed from around the delicate embossed features. However, with the exception of the glossy XY specimens, all specimens require cleaning after printing (for consistency, the glossy XY specimens were cleaned as well, even though they had no support material). This means that it is impossible to tell the “true” minimum manufacturable feature size, since it is always possible that features will break during cleaning. Because of this, the next section (Section 5) will present experiments where different features were placed under load by the waterjet to determine the variables that affect a feature’s ability to survive the cleaning process.

5. SURVIVABLE FEATURE SIZE

5.1. Motivation

An interesting additional consideration for the PolyJet process is that, while the system may be able to reproduce a feature of an incredibly small size (as shown in the minimum resolvable feature size specimens), the feature may be broken while using the water jet to clean the part. This has already been alluded to with the long, thin arms and displacement tip on the two printed inverters shown earlier in Figure 2. To ensure that a part can survive the cleaning process, it may be necessary for the smallest

printed feature to be larger than what the machine’s smallest resolvable feature size actually is. This section will focus on determining the variables that have a dominant effect on the survivability of any printed parts

The experiments described in this section are designed to answer the question, *What process parameters and geometric features affect the smallest part feature size that can be cleaned without breaking?*

5.2. Experimental Methods

The same rig from the support cleaning tests is used to determine the factors which affect minimum survivable feature size. However, the geometry of the specimens, and thus the specimen holder, differs slightly. For this experiment, the feature under testing is kept simple; initial focus will be on investigating a beam-like feature, since this compares well to the geometry of the minimum feature specimens and the printed compliant inverters. The independent variables under investigation include (i) feature cross-sectional area, (ii) feature length, (iii) build material, and (iv) connectivity (e.g., cantilevered at one end or fixed at both ends). These variables will allow us to gain a general understanding of which factor most drives breakage during cleaning. Note that in this experiment, the variable “length” simply refers to the distance between the two ends of the printed feature.

Representative specimens are shown in Figure 9. Survivability is considered binary (either the feature broke after the allotted 1-minute cleaning time or it did not break). This experiment differs slightly from the previous ones; a full factorial experiment of these three variables was performed twice: once using VW+ for all of the tests and once using TB+ for all tests. The variables, their possible states, and the hypothesis for each are collected in Table 7.

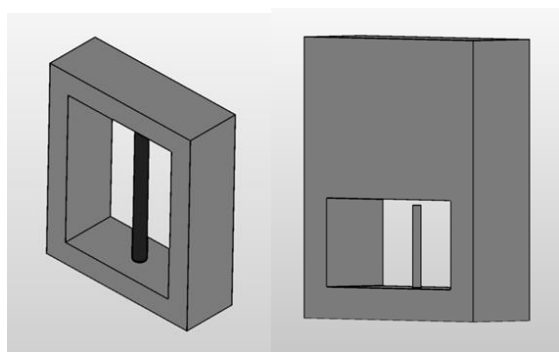


Figure 9. Example of Cleaning Survivability Test Specimens

Table 7. Experimental Variables for Survivable Feature Size

Independent Variables			
<i>Variable Name</i>	<i>State 1</i>	<i>State 2</i>	<i>Rationale/Hypothesis</i>
Connectivity	Fixed	Cantilevered	Having the feature cantilevered at only one end would result in a higher reaction load at that point, increasing the shear stress and the likelihood of part breakage at the joint.
Cross-Sectional Area	0.75 mm	1.50 mm	A smaller cross-sectional area will result in larger stresses in the feature due to the force of cleaning, which would again increase the likelihood of breakage.
Length	17.00 mm	6.86 mm	Having a longer specimen should increase the length of the moment arm at the fixation points due to the force of the waterjet. This will increase the normal stresses at the joint and increase potential for breakage.
Dependent Variable			
<i>Variable Name</i>	<i>Units</i>		<i>Rationale</i>
Survivability	Yes or No		Measuring survivability (in simple yes/no terms) will help to determine the variables that determine if a particular element in a final design will be able to survive the cleaning process.

5.3. Results

The survivability specimen experimentation was first performed for 8 combinations of the main factors for VW+ material (based on an L8 Taguchi array). The results from the ANOVA analysis of this experimentation are as follows. Note that a score of 2 denotes a survivable feature, while a score of 1 denotes a broken specimen. The mean response of 1.438 in Table 8 shows that approximately 44% of the tested VW+ specimens fractured under the waterjet loading (a value of 1.000 would mean that all specimens broke). However, as the p-values in Table 9 demonstrate, almost all of the broken specimens are due to the cross-sectional area (p-value of 0.002). The desirability predictions in Figure 10 reinforce this notion; the predictions recommend a large cross-section along with fixed connectivity and a long length to minimize VW+ specimen breakage (though, as already mentioned, the effects of connectivity and length are not statistically significant).

Table 8. Summary of Fit – Survivable Feature Size

RSquare	0.927
Root Mean Square Error	0.177
Mean of Response	1.438
Observations (or Sum Wgts)	8

Table 9. Parameter Estimates – Survivable Feature Size

Term	Estimate	Std Error	t Ratio	Prob> t
Intercept	1.438	0.063	23.00	<.001*
Connectivity[Cantilevered]	-0.063	0.063	-1.00	0.374
Cross-Sectional Area[Large]	0.438	0.063	7.00	0.002*
Length[Long]	0.063	0.063	1.00	0.374

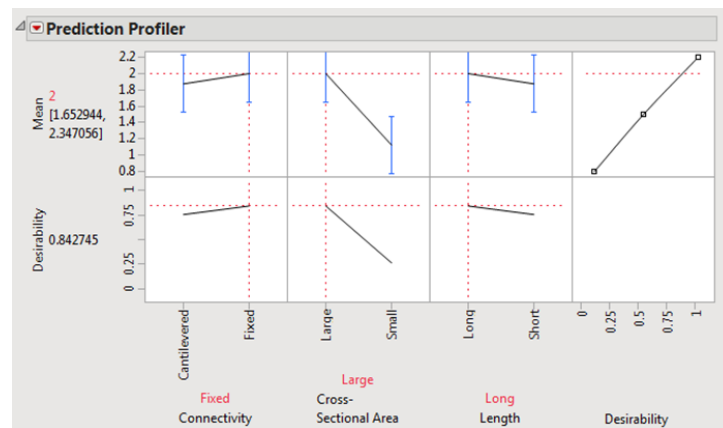


Figure 10. Desirability Prediction – Survivable Feature Size

After performing the experiment with VW+ material, the same 8 combinations were printed using TB+ material. When tested, every cantilevered TB+ specimen survived cleaning while every specimen fixed at both ends broke, regardless of length or cross-sectional area. This shows that connectivity should be the only significant independent variable when considering survivability of TB+ material. This differs from the VW+ specimens, which break almost entirely due to the specimen's cross-sectional area.

5.4. Discussion

The differing results between VW+ and TB+ specimens makes intuitive sense. For the more rigid VW+ material, thin features will not flex under the load of the water jet. Because of this, the cross-sectional area dominates whether a feature will survive, with larger areas experiencing lower shear stress from the waterjet load. This gives them a higher chance for survival (in the case of this experimentation,

a diameter of 1.5 mm was consistently able to survive cleaning). On the other hand, when cantilevered, the elastomeric nature of the TB+ material causes it to flex under the water jet instead of fracturing. When the load is removed, the flexible material rebounds to its original position. When the TB+ specimen is fixed at both ends, it is unable to freely deflect and instead ruptures at the point of loading.

6. SELF-SUPPORTING ANGLE

6.1. Motivation

While the PolyJet process in its default configuration relies on the use of support material for any constructed angle (save for perfectly vertical faces), it is possible to turn off the use of support material in the system completely. This would allow a designer to create a specimen, such as the inverters from Figure 2, without worrying about 1) whether or not the triangular holes could be cleaned easily or 2) whether or not the waterjet would cause the fragile arms of the inverter to break. To take full advantage of this feature, it is important to know how certain process variables affect the self-supporting angle when support material has been eliminated. By knowing understanding these effects, a designer could be confident that angled surfaces from a TO algorithm (such as the surface highlighted with a dashed line in Figure 2) could be created properly without compromising the geometry of the final part or the safety of the machine.

The experiments described in this section are designed to answer the questions, *What process parameters affect the most acute angle that can be created in the absence of support material?*

6.2. Experimental Methods

A simple specimen consisting of 10 faces at steadily increasing angles was designed to quantify the self-supporting angle of PolyJet parts when support material is turned off. The two independent variables under investigation are (i) material choice and (ii) orientation of the angled face with respect to the printhead's roller. Orientation is tested to determine if the roller is potentially pushing deposited droplets off of the self-supporting edge. If the roller is pushing droplets, this could result in a poorer self-supporting angle when the motion of the roller is perpendicular to the front edge of the specimen instead of parallel. The specimen used for testing (seen in Figure 11) contains 10 faces, starting from a vertical 90 degree face (measured from the horizontal) and moving to a 72 degree face in 2 degree increments. The candidate orientations are 1) with the specimen's longest dimension aligned in the x-direction and 2) with the specimen's longest dimension aligned in the y-direction. These variables are collected in Table 10 along with their associated hypotheses. Each possible combination of variables was tested twice.

Table 10. Experimental Variables in Self-Supporting Angle

Independent Variables			
Variable Name	State 1	State 2	Rationale/Hypothesis
Material Type	TB+	VW+	The compressive force of the roller may deform the flexible TB+ material during printing, causing fresh droplets to fall off the upper surface. If the material droplets have different viscosity properties, then one may be able to support higher angles than the other.
Orientation	X-Dominated	Y-Dominated	The roller may be pushing droplets off of the edge, which could result in a poorer self-supporting angle for a specimen predominantly oriented in the y-direction.
Dependent Variable			
Variable Name	Units	Rationale	
Self-Supporting Angle	Degrees (from Horizontal)	Measuring the self-supporting angle with the given independent variables will show the recommended angle, orientation, and material type for printing optimized parts without support material.	

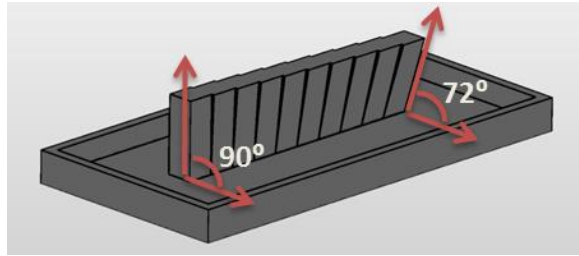


Figure 11. Self-Supporting Angle Specimen

6.3. Results

Experimentation shows that all specimens failed before the final 72 degree angled face. This failure is shown through stalagmites that appear to grow right beneath the angled face (an example is shown in Figure 12).



Figure 12. Stalagmites Denote a Non-Self-Supporting Angled Face

The maximum self-supporting angle was determined to be at the face before significant stalagmite growth was shown. The maximum angle was recorded for each of the 8 printed specimens. ANOVA analysis was performed on a full-factorial array to determine which of the factors, if any, had a significant effect on the maximum self-supporting angle.

The mean benchmark self-supporting angle for all specimens is 84.5 degrees from horizontal (see Table 11). Again, this average value accounts for changes in both independent variables. From this analysis, it appears that material choice ($p = 0.205$) does not have a statistically significant effect ($p < 0.05$) on the maximum self-supporting angle (shown in Table 12). However, there does seem to be a potential pattern related to orientation that may merit further investigation with more test iterations ($p = 0.064$); the mean angle for the x-dominated specimens was 87 degrees from horizontal while the mean angle for y-dominated specimens was 82 degrees. While the p-value in Table 12 does not confirm statistical significance, more specimen iterations may decrease the standard deviation in the orientation data and better show if orientation has a significant effect. Based on the desirability predictions from this experiment (seen in Figure 13), the best self-supporting angle would be achieved on a specimen with TB+ material oriented in the y-direction.

Table 11. Summary of Fit – Self-Supporting Angle

RSquare	0.991
Root Mean Square Error	0.5
Mean of Response	84.5
Observations (or Sum Wgts)	4

Table 12. Parameter Estimates – Self-Supporting Angle

Term	Estimate	Std Error	t Ratio	Prob> t
Intercept	84.5	0.25	338.00	0.002*
Material[TB+]	-0.75	0.25	-3.00	0.205
Orientation[X-Dominated]	2.5	0.25	10.00	0.064

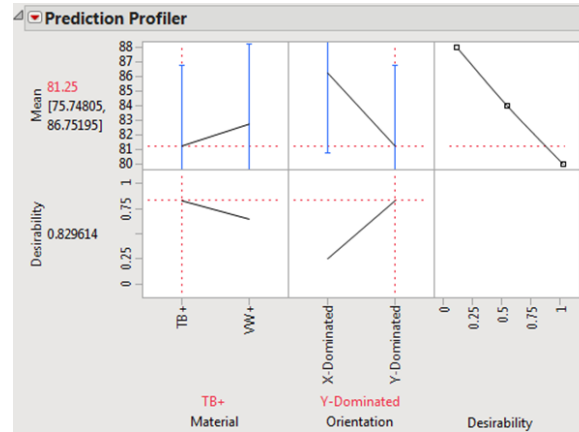


Figure 13. Desirability Prediction – Self-Supporting Angle

6.4. Discussion

It is worth noting that the desirability predictions in Figure 13 are directly contrary to the initial hypothesis that specimens oriented in the x-dominated direction would see a better self-supporting angle. This data suggests that having the roller passing over the material droplets in the direction of the angled face’s leading edge is actually beneficial. Unfortunately, the authors cannot offer a concrete hypothesis at this time as to why this may be the case (though it is possible that it could be connected either to the presence of the roller or to the nature of the material jetting from the nozzles). Also, while the predictions recommend the TB+ material over the VW+, there is no statistically significant evidence from this testing to confirm that it would truly offer a better self-supporting angle.

7. CONCLUSIONS AND RECOMMENDATIONS FOR FUTURE WORK

This work presents a series of designed experiments to determine the key parameters that influence four specific manufacturing considerations in the PolyJet process. The variables that affect minimum feature size, support material removal, feature survivability, and self-supporting angles are identified as follows:

- Support material removal experimentation demonstrated a reliance solely on the cross-sectional area of the channel.
- The minimum resolvable feature size has been shown to rely on material choice and feature direction.
- Feature survivability during cleaning was tied to cross-sectional area (for VW+ features) and feature connectivity (for TB+ features).
- Finally, the self-supporting angle in the absence of support material was driven by the orientation of the surface with respect to the roller, with y-dominated specimens offering better self-supporting angles.

Identifying these key variables is a crucial to incorporating PolyJet manufacturing considerations into TO methods. Future work will focus on 1) establishing clear quantitative relationships between the key factors identified in this paper and their associated dependent variables, 2) determining the lower limits of

the dependent variables due to the effects of the key factors, and 3) investigating manufacturing considerations that arise specifically when printing stiff and flexible materials in a monolithic structure. This will include investigation of the material properties in the interface regions between disparate material elements as well as a quantifying the effects of changing feature size on digital material properties.

8. REFERENCES

- [1] Brackett, D., Ashcroft, I., and Hague, R., 2011, "Topology Optimization for Additive Manufacturing," 22nd Annual International Solid Freeform Fabrication Symposium, pp. 348–362.
- [2] Watts, D. M., and Hague, R., 2006, "Exploiting the Design Freedom of RM," 17th Annual International Solid Freeform Fabrication Symposium, pp. 656–667.
- [3] Graf, G. C., Chu, J., Engelbrecht, S., and Rosen, D. W., 2009, "Synthesis Methods for Lightweight Lattice Structures," ASME 2009 International Design Engineering Technical Conferences and Computers and Information in Engineering Conference, ASME, pp. 579–589.
- [4] Rosen, D. W., 2007, "Computer-Aided Design for Additive Manufacturing of Cellular Structures," *Comput. Aided. Des. Appl.*, **4**(5), pp. 585–594.
- [5] Hascoet, J. Y., Ponche, R., Kerbrat, O., and Mognol, P., 2012, "From Functional Specifications to Optimized CAD Model : Proposition of a New DFAM Methodology," *Innov. Dev. Virtual Phys. Prototyp.*, pp. 467–472.
- [6] Ponche, R., Kerbrat, O., Mognol, P., and Hascoet, J. Y., 2013, "Consideration of the Manufacturing Trajectories in a Global Design for Additive Manufacturing Methodology," ASME 2012 Biennial Conference on Engineering Systems Design and Analysis, pp. 1–9.
- [7] Harzheim, L., and Graf, G., 2005, "A Review of Optimization of Cast Parts Using Topology Optimization: I - Topology Optimization without Manufacturing Constraints," *Struct. Multidiscip. Optim.*, **30**(6), pp. 491–497.
- [8] Harzheim, L., and Graf, G., 2005, "A Review of Optimization of Cast Parts using Topology Optimization: II - Topology Optimization with Manufacturing Constraints," *Struct. Multidiscip. Optim.*, **31**(5), pp. 388–399.
- [9] Maidin, S. Bin, 2011, "Development of a Design Feature Database to Support Design for Additive Manufacturing," Loughborough University.
- [10] Seepersad, C. C., Govett, T., Kim, K., Lundin, M., and Pinerio, D., 2012, "A Designer's Guide for Dimensioning and Tolerancing SLS parts," 23rd Annual International Solid Freeform Fabrication Symposium, pp. 921–931.
- [11] Schevenels, M., Lazarov, B. S., and Sigmund, O., 2011, "Robust Topology Optimization Accounting for Spatially Varying Manufacturing Errors," *Comput. Methods Appl. Mech. Eng.*, **200**(49-52), pp. 3613–3627.
- [12] Guest, J. K., Prévost, J. H., and Belytschko, T., 2004, "Achieving Minimum Length Scale in Topology Optimization Using Nodal Design Variables and Projection Functions," *Int. J. Numer. Methods Eng.*, **61**(2), pp. 238–254.
- [13] Meisel, N. A., Gaynor, A., Williams, C. B., and Guest, J. K., 2013, "Multiple-Material Topology Optimization of Compliant Mechanisms Created via PolyJet 3D Printing," 24th Annual International Solid Freeform Fabrication Symposium, pp. 980–997.
- [14] Stratasys, 2013, "Objet 350 Connex: Build Mid-Size Prototypes in Multiple Materials" [Online]. Available: <http://stratasys.com/3d-printers/design-series/precision/objet-connex350>.
- [15] Moore, J. P., and Williams, C. B., 2008, "Fatigue Characterization of 3D Printed Elastomer Material," Solid Freeform Fabrication Symposium, pp. 641–655.
- [16] Pilipović, A., Raos, P., and Šercer, M., 2007, "Experimental Analysis of Properties of Materials for Rapid Prototyping," *Int. J. Adv. Manuf. Technol.*, **40**(1-2), pp. 105–115.

- [17] Vieira, L. F., and Paggi, R. A., 2012, "Thermal and Dynamic-Mechanical Behavior of Fullcure 3D Printing Resin Post-Cured by Different Methods," *Innov. Dev. Virtual Phys. Prototyp.*, pp. 385–388.
- [18] Gibson, I., Goenka, G., Narasimhan, R., and Bhat, N., 2010, "Design Rules for Additive Manufacture," *Solid Freeform Fabrication Symposium*, pp. 705–716.
- [19] Udriou, R., and Mihail, L., 2009, "Experimental Determination of Surface Roughness of Parts Obtained by Rapid Prototyping," 8th WSEAS International Conference on Circuits, Systems, Electronics, Control and Signal Processing, pp. 283–286.
- [20] Udriou, R., and Nedelcu, A., 2011, "Optimization of Additive Manufacturing Processes Focused on 3D Printing," *Rapid Prototyp. Technol. -- Princ. Funct. Requir.*, pp. 1–28.
- [21] Singh, R., 2011, "Process Capability Study of Polyjet Printing for Plastic Components," *J. Mech. Sci. Technol.*, **25**(4), pp. 1011–1015.
- [22] Singh, R., and Singh, V., 2011, "Experimental Investigations for Rapid Moulding Solution of Plastics Using Polyjet Printing," *Mater. Sci. Forum*, **701**, pp. 15–20.
- [23] Kim, G. D., and Oh, Y. T., 2008, "A Benchmark Study on Rapid Prototyping Processes and Machines: Quantitative Comparisons of Mechanical Properties, Accuracy, Roughness, Speed, and Material Cost," *Proc. Inst. Mech. Eng. Part B J. Eng. Manuf.*, **222**(2), pp. 201–215.
- [24] Vayre, B., Vignat, F., and Villeneuve, F., 2012, "Designing for Additive Manufacturing," *Procedia CIRP*, **3**, pp. 632–637.
- [25] Vayre, B., Vignat, F., and Villeneuve, F., 2013, "Identification on Some Design Key Parameters for Additive Manufacturing: Application on Electron Beam Melting," *Procedia CIRP*, **7**, pp. 264–269.
- [26] Moylan, S., Slotwinski, J., Cooke, A., Jurens, K., and Donmez, M. A., 2012, "Proposal for a Standardized Test Artifact for Additive Manufacturing Machines and Processes," *Solid Freeform Fabrication Symposium*, pp. 902–920.